Dependence of Transport Properties of Concentrated Lithium Salt Solutions on Temperature and Composition in an Imidazolium-Based Liquid Zwitterion Containing an Oligo(Ethylene Oxide) Unit

Mitsutake Suematsu, Masahiro Yoshizawa-Fujita[*], Tetsuya Tamura, Yuko Takeoka, Masahiro Rikukawa

Department of Materials and Life Sciences, Sophia University, 7-1 Kioi-cho, Chiyoda-ku, Tokyo 102-8554, Japan.
[*]E-mail: masahi-f@sophia.ac.jp

In order to investigate the effects of lithium salt species and concentration on the electrochemical properties of a liquid zwitterion (LZw), composites of a LZw with lithium bis(fluorosulfonyl)amide (LiFSA) or lithium bis(trifluoromethylsulfonyl)amide $(LiN(Tf)_2)$ were prepared at various lithium salt concentrations. The majority of LZw/LiFSA and $LZw/LiN(Tf)_2$ composites with lithium salt mole fractions in the range of 0.2 to 0.8 were obtained as colorless liquids and exhibited glass transitions only during DSC measurements. The dissociation state of the lithium salts in the composites was discussed by means of FT-IR measurements. The interactions between the imidazolium cation and the amide anions were demonstrated. The LZw/LiFSA composite with a LiFSA mole fraction of 0.8 (corresponding to a concentration of 13.7 mol kg^{-1}) exhibited the highest ionic conductivity (1.2×10^{-5} S cm^{-1}) as well as the greatest lithium transference number (0.46) at 40°C.

1. INTRODUCTION

Ionic liquids (ILs) are promising candidates as electrolytes for use in lithium-ion secondary batteries, due to properties such as low volatility, non-flammability, high ionic conductivity, and electrochemical stability, all of which are important for the safety and performance of electronic devices [1-5]. Using ILs as electrolyte solutions is challenging, however, because their component ions can migrate under a potential gradient, resulting in low lithium transference numbers [6]. To overcome this obstacle, new matrices capable of selectively transporting the appropriate carrier ions need to be

designed.

Zwitterions have been considered as possible selective transport compounds. Since these molecules contain both cationic and anionic charges, their migration under a potential gradient should be minimal [7,8]. Organoborate zwitterion/lithium bis(trifluoromethylsulfonyl)amide (LiN(Tf)$_2$) composites have been shown to possess a high lithium transference number (t_{Li+}) greater than 0.60 [9], although achieving both a high t_{Li+} value and good ionic conductivity remains difficult.

A previous study reported that an imidazolium-based zwitterion containing two oxyethylene units (LZw) was synthesized as a colorless liquid at room temperature [10]. An equimolar mixture of LZw with LiN(Tf)$_2$ had an ionic conductivity value superior to those of solid zwitterion/LiN(Tf)$_2$ composites. In the present study, the use of lithium bis(fluorosulfonyl)amide (LiFSA) was investigated to achieve further improvements in conductivity. ILs that incorporate the FSA anion exhibit higher ionic conductivities and lower viscosities compared to ILs with the N(Tf)$_2$ anion [11-15] and improve battery performance when employed in Li/LiCoO$_2$ [12] or graphite negative electrode cells compared to N(Tf)$_2$-based ILs [13,16].

2. EXPERIMENTAL

2.1. Materials
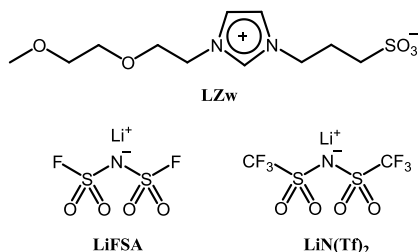
Figure 1. Molecular structures of LZw, LiFSA, and LiN(Tf)$_2$.

In this work, the LZw was synthesized according to a previously published procedure [10]. Water content of the LZw, as measured by Karl-Fischer moisture titration, was less than 10 ppm (average of three readings). The LiN(Tf)$_2$ (Morita Chemical Co., Ltd., 99.9%) and LiFSA (Piotrek, 99.0%) were used as received without further purification. The chemical structures of LZw, LiN(Tf)$_2$, and LiFSA are shown in Fig. 1. LZw was mixed with the chosen lithium salt in a glove box under an argon atmosphere. The resulting mixture was stirred at 60ºC for 24 h to obtain the desired LZw/LiX (*x*), where X and *x* represent the amide anion and mole fraction of the lithium salt, respectively.

2.2. Methods

Thermogravimetric analysis was conducted using a TG-DTA instrument (TG-DTA7200, Hitachi High-Technologies Corp.) under a nitrogen atmosphere at temperatures from 25 to 500°C at a

heating rate of 10ºC min^{-1}. Thermal behavior was examined using a differential scanning calorimetry (DSC) (DSC7020, Hitachi High-Technologies Corp.) at temperatures between -150 and 150°C (LZw/LiFSA) or 100°C (LZw/LiN(Tf)$_2$) at a heating/cooling rate of 10°C min^{-1}.

The cyclic voltammetric measurements of 0.05 M of LZw/Li salt composites in acetonitrile solutions at room temperature were performed using a potentiostat/galvanostat (ALS Model 660B, BAS Inc.) with a glassy carbon working electrode (3 mm in diameter) used with a platinum wire as a counter electrode and a silver wire immersed in an Ag/AgNO$_3$ acetonitrile solution as a reference electrode. All potentials are reported versus the ferrocene/ferrocenium half potential. Scan rate and temperature were 10 mV s^{-1} and 25°C under an argon atmosphere. The temperature was controlled using a constant temperature oven (TB-1, BAS Inc.).

Ionic conductivity measurements were conducted using a stainless steel cell (TYS-00DM01, Toyo System Co., Ltd.). Samples were placed between two platinum electrodes polished with 1.0, 0.3, and 0.05 μm Al$_2$O$_3$ powder and their ionic conductivity obtained by measuring the complex impedance of the cell between 5 Hz and 1 MHz using an impedance analyzer (1260, Solatron) over the temperature range of 25 to 80ºC. The temperature was controlled using a constant temperature oven (SH-241, Espec Corp.). To determine the carrier ion species in the composites, the lithium transference number (t_{Li+}) values were estimated using a combination of AC impedance and DC polarization with lithium metal electrodes at 40°C, which was precisely controlled using a constant temperature oven (TB-1, BAS Inc.) at a potential bias of 10 mV [17].

3. RESULTS AND DISCUSSION
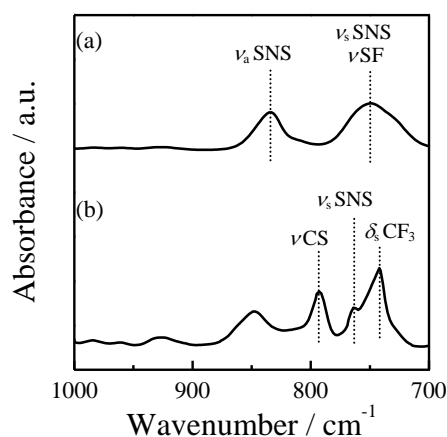
Figure 2. FT-IR spectra of (a) LZw/LiFSA (0.5) and (b) LZw/LiN(Tf)$_2$ (0.5) composites (ν, stretching; δ, bending).

LZw/LiFSA and LZw/LiN(Tf)$_2$ composites with lithium salt mole fractions in the range of 0.2 to 0.8 were obtained as colorless liquids, with the exception of the LZw/LiN(Tf)$_2$ composites for which *x* was 0.6 and 0.7; these were crystallized over a period of several days. At a lithium salt mole fraction of 0.9, both composites were obtained as solids at room temperature. FT-IR spectra were obtained to

investigate the dissociation state of the lithium salts in the composites. Fig. 2 shows the FT-IR spectra of both LZw/LiX (0.5) composites. The S-N-S stretching vibration peaks [symmetric stretching mode (ν_s SNS) and asymmetric stretching mode (ν_a SNS)] of the FSA anion in the composite were observed at 749 cm^{-1} and 834 cm^{-1}, respectively. The broad peak at 749 cm^{-1} in the spectrum of the LZw/LiFSA composite contained the response of ν SF [18]. The corresponding peaks of LiFSA occurred at 759 cm^{-1} and 870 cm^{-1} [18]. The ν_s SNS of the N(Tf)$_2$ anion in the composite was observed at 763 cm^{-1}. The corresponding peak of LiN(Tf)$_2$ has been reported to occur at 770 cm^{-1} [19]. These data indicate that the combination of the lithium salts with LZw shifted these peaks to lower wavenumbers as the result of interactions between the imidazolium cation and amide anions. Similar interactions in zwitterion/LiN(Tf)$_2$ composites have been described [19]. Another indication of these interactions is the observation that zwitterions are capable of dissolving many different inorganic salts [8,20].
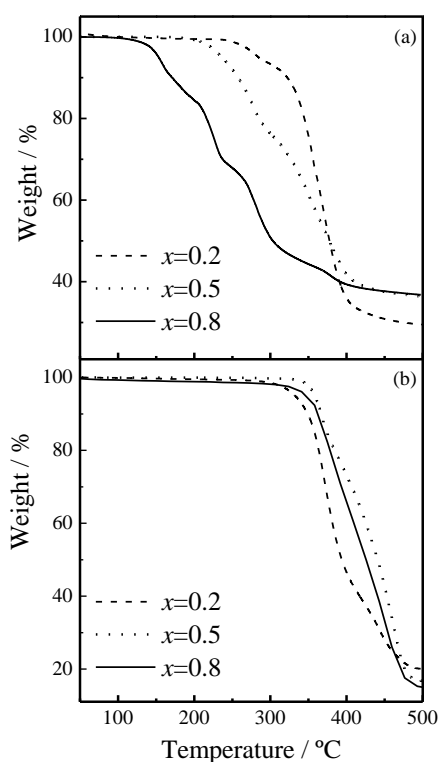
Figure 3. TG curves of (a) LZw/LiFSA (0.2, 0.5 and 0.8) and (b) LZw/LiN(Tf)$_2$ (0.2, 0.5 and 0.8).

The TG plots obtained for LZw/LiX (x = 0.2, 0.5, and 0.8) composites are shown in Fig. 3. Thermal decomposition onset temperature (T_d) values for the LZw/LiN(Tf)$_2$ composites were all above 300°C, while the T_d values of the LZw/LiFSA (0.2) and (0.5) composites occurred at approximately 250 and 200°C, respectively. When the mole fraction of the lithium salt was less than 0.5, T_d values of the composites were very similar to that of pure LZw (317°C) [10]. The T_d values of both LZw/LiX (0.5) composites were equal to those reported for ILs composed of an imidazolium cation and either the N(Tf)$_2$ or FSA anion [18,21]. When the mole fraction of the lithium salt was greater than 0.6, the LZw/LiX composites exhibited T_d values equal to those of their pure lithium salts, suggesting that the

FSA and $N(Tf)_2$ anions interacted primarily with the LZw imidazolium cation at mole fractions less than 0.5.

The DSC traces of the composites are presented in Fig. 4. Only those composites with lithium salt mole fractions between 0.2 and 0.8 exhibited a glass transition. Fig. 5 summarizes the relationship between glass transition temperature (T_g) and lithium salt concentration. At mole fractions less than 0.5, both composites have similar T_g values, which are nearly equal to that of pure LZw. The T_g values of both composites increased with a mole fraction greater than 0.6.
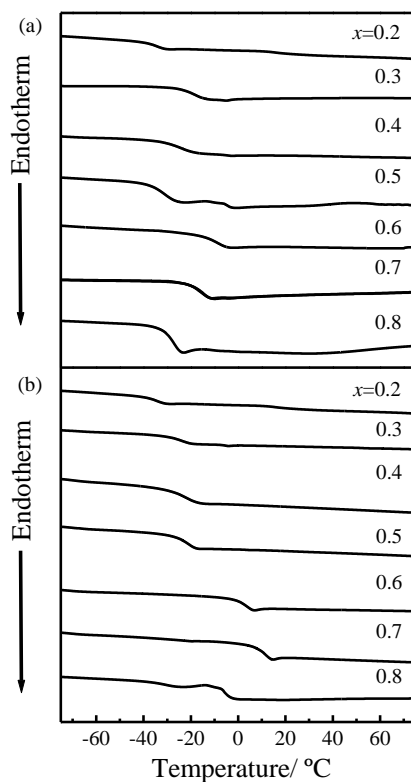

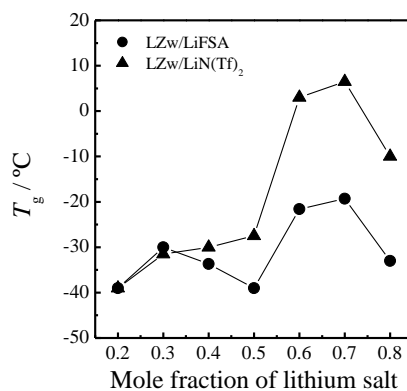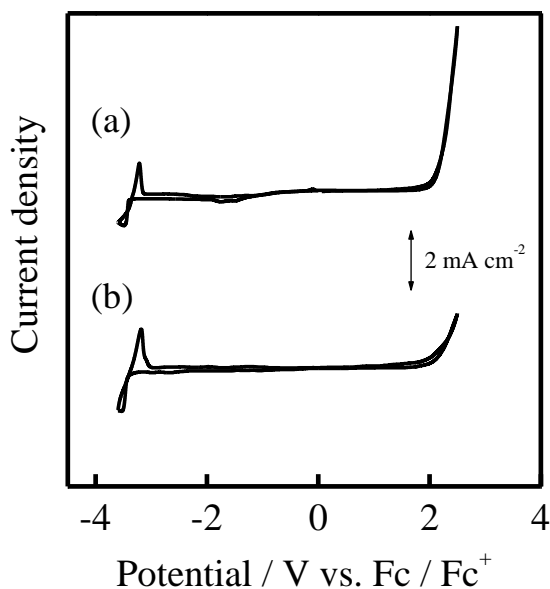**Figure 4.** DSC curves of (a) LZw/LiFSA and (b) LZw/LiN(Tf)$_2$ composites.

Figure 5. Relationship between T_g and mole fraction of the lithium salt in LZw/LiX composites.

The LZw/LiFSA composites produced lower T_g values compared to the LZw/LiN(Tf)$_2$ composites and had glass transitions at temperatures below -20°C over the range of x from 0.2 to 0.8. The T_g values of both LZw/LiX (0.8) composites were less than those of the corresponding LZw/LiX (0.6) and (0.7) composites, and the LZw/LiN(Tf)$_2$ (0.8) composite maintained an amorphous state even though the LZw/LiN(Tf)$_2$ (0.6) and (0.7) materials transitioned to the solid state after several days. Both LZw/LiX (0.9) composites were solids at room temperature; the melting point (T_m) of the LZw/LiN(Tf)$_2$ (0.9) composite was 217°C while the LZw/LiFSA (0.9) composite decomposed before melting.

Fig. 6 shows the cyclic voltammograms of the LZw/LiFSA (0.5) and LZw/LiN(Tf)$_2$ (0.5) composites in acetonitrile at room temperature. Electrochemical stability is a key feature for the application of LZw in electrochemical devices. The reduction and oxidation potentials were −3.5 V and 2.0 V, respectively, *vs.* Fc/Fc$^+$ providing an electrochemical window greater than 5 V. The electrochemical stability of both composites was almost the same regardless of lithium salt species. The voltammogram indicated that those composites possessed good electrochemical stability, similar to those of ILs with N(Tf)$_2$ anion [1].

Figure 6. Cyclic voltammograms of 0.05 M acetonitrile solutions of (a) LZw/LiFSA (0.5) and (b) LZw/LiN(Tf)$_2$ (0.5) at 10 mV s^{-1} on glassy carbon at room temperature.

Fig. 7 shows the ionic conductivity of LZw/LiFSA and LZw/LiN(Tf)$_2$ composites as a function of temperature (as Arrhenius plots). An upward convex curve was observed in these plots for all of the composites used in this study, suggesting that the ion conductive process can be expressed by the Vogel-Fulcher-Tamman (VFT) equation [22], which describes the temperature dependence of viscosity in amorphous materials.
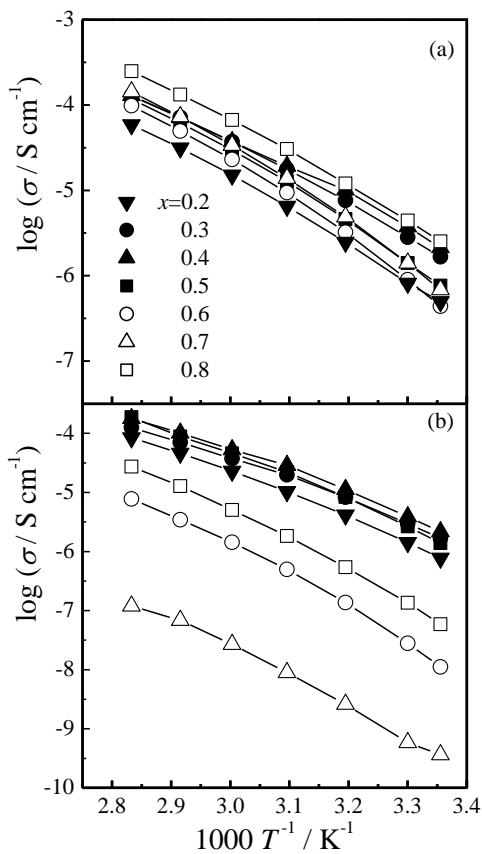
Figure 7. Ionic conductivity of (a) LZw/LiFSA and (b) LZw/LiN(Tf)$_2$ as a function of temperature.
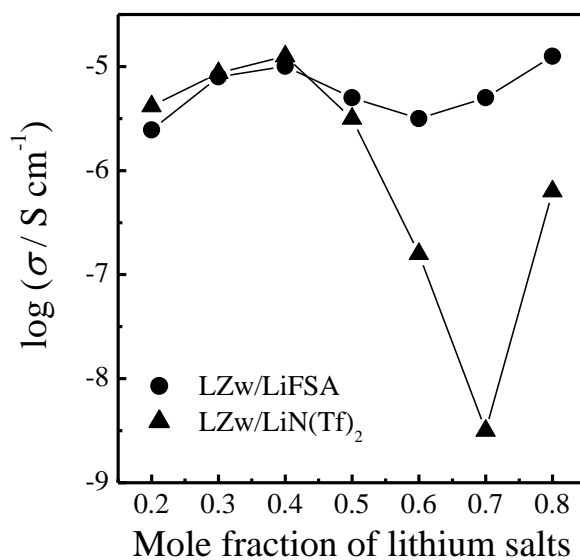

Figure 8. Effect of mole fraction of the lithium salt on ionic conductivity at 40°C for LZw/LiX composites.

Fig. 8 shows the plots of lithium salt concentration *vs.* ionic conductivity of the LZw/LiX composites at 40°C. Conductivities of all of the LZw/LiN(Tf)$_2$ ($x \leq 0.5$) composites were in the range of 10^{-5} to 10^{-6} S cm^{-1}, while the LZw/LiN(Tf)$_2$ ($x \geq 0.6$) composites had values less than 10^{-6} S cm^{-1} due to an increase in T_g values with lithium salt concentrations. Good correlation between ionic conductivity and T_g values was found for ILs [23]. The ionic conductivities of the LZw/LiFSA ($x = 0.2$ - 0.8) composites were in the range of 10^{-5} to 10^{-6} S cm^{-1}, regardless of lithium salt concentration. The LZw/LiFSA (0.8) composite possessed the highest ionic conductivity (1.2×10^{-5} S cm^{-1}) of all of the materials tested.

As noted, the LZw/LiFSA (0.8) composite had the highest ionic conductivity among the LZw/LiFSA composites. The molality of this composite was 13.7 mol kg^{-1}. Previous studies of typical ILs in battery applications have used much lower lithium salt concentrations, *e.g.*, in the range of 0.3 to 0.5 mol kg^{-1} [12,13,16], because the addition of lithium ions both decreases ionic conductivity and increases viscosity due to the strong electrostatic interactions of the lithium ion [6a,24,25]. The dependence of ionic conductivity of these LZw/LiFSA composites on the lithium salt concentration is atypical, especially when compared to behavior exhibited between standard organic solvents and ILs. Ionic conductivity decreases monotonically with increasing T_g in many different ion conductive matrices as a result of a decrease in molecular motion induced by increased T_g. The ion conduction in these electrolytes is associated with the molecular motion of solvent molecules [26], while the ion conduction in LZw/LiFSA composites decouples conduction from the migration of the LZw. Angell *et al.* reported that addition of a small amount of poly(propylene oxide) to LiAlCl$_4$, to produce a polymer-in-salt, was an effective way to obtain a high t_{Li+} value and good ionic conductivity [27]. The LZw/LiFSA composites used here achieved their highest levels of conductivity at the highest mole fraction of LiFSA, similar to the 'polymer-in-salt' phenomenon. These LZw/LiFSA composites therefore represent a decoupled electrolyte.
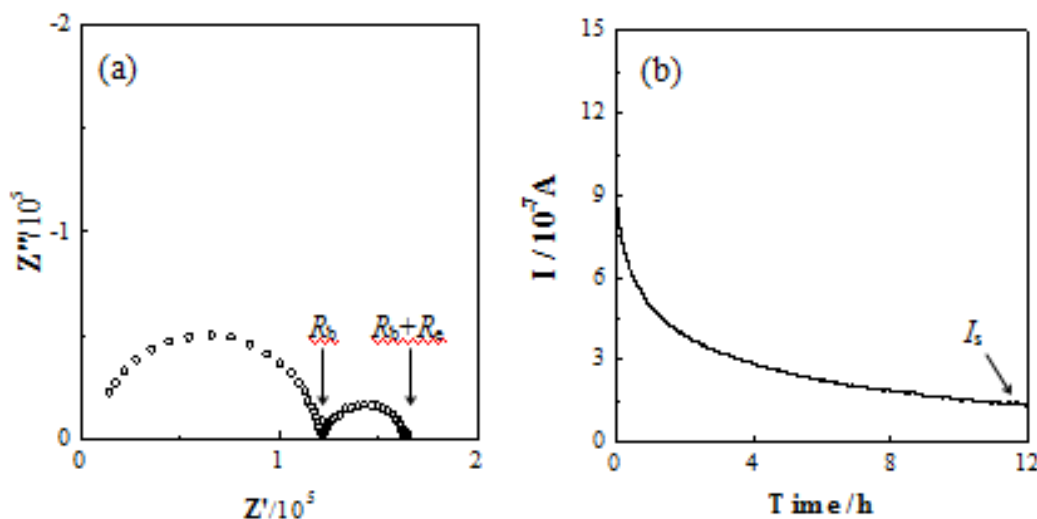
Figure 9. Nyquist plot (a) and time dependence of direct current polarization curve at 10 mV (b) for LZw/LiN(Tf)$_2$ (0.5). R_b: bulk resistance, R_e: interfacial resistance, I_s: steady current.

The t_{Li+} values of the LZw/lithium salt composites were obtained to estimate the carrier ion species in the materials. The t_{Li}^+ values were determined according to the method reported by Ogata and co-workers [17]. The bulk and interface resistances were determined by the complex impedance measurements. Figs. 9 shows the Nyquist plot and time dependence of direct current polarization curve for LZw/LiN(Tf)$_2$ (0.5) as the representative. Table 1 summarizes the t_{Li+} values of LZw/LiX composites at 40°C. Since the t_{Li+} values of the LZw/LiX ($x \leq 0.3$) composites were less than 0.10, exact values could not be obtained by this method [17]; thus, the figures in this table for those materials are approximations.

Table 1. t_{Li+} values of LZw/Li salt composites at 40°C

Mole fraction of Li salt	t_{Li+}	
	LiFSA	LiN(Tf)$_2$
0.8	0.46	-[a]
0.7	0.44	-[b]
0.6	0.14	-[b]
0.5	0.20	0.15
0.3	0.07	0.02

[a] Not obtained. [b] Not measured

The t_{Li+} values of LZw/LiFSA (0.5) and (0.8) were 0.20 and 0.46, respectively, and the LZw/LiN(Tf)$_2$ (0.5) value was 0.15, while the t_{Li+} of LZw/LiN(Tf)$_2$ (0.8) could not be calculated, because the bulk resistance was so great that the interface resistance could not be measured. All of the LZw/LiFSA composites had greater t_{Li+} values than the LZw/LiN(Tf)$_2$ composites, due to lower coordination strength between the FSA anion and Li$^+$ compared with that of the N(Tf)$_2$ anion [11]. Even though the ionic conductivity values of the LZw/LiFSA composites were similar, the t_{Li+} of the LZw/LiFSA (0.8) material was greater than those of the LZw/LiFSA (0.5), (0.6), and (0.7) composites; thus, the trend of the t_{Li+} values of the LZw/LiFSA ($x \geq 0.5$) composites was similar to that of ion conductivity. The interaction between the lithium ions and ether units of the imidazolium cation could represent an effective ion conductive pathway in these composites and has been considered an important factor in electrochemical properties [28].

4. CONCLUSIONS

Composites consisting of a liquid zwitterion with one of two different lithium salt species (LiFSA and LiN(Tf)$_2$) were prepared, and the effects of the lithium salt and concentration on thermal and electrochemical properties of the composite were evaluated. The majority of the LZw/lithium salt composites were viscous liquids at room temperature and exhibited glass transitions only during DSC measurements, with the LZw/LiFSA composites showing particularly low T_g values, all of which were

below -20°C. The LZw/LiFSA (0.8) composite exhibited the greatest ionic conductivity values and lithium transference number (t_{Li+}), indicating that the FSA anion effectively improved the electrochemical properties of the LZw/lithium salt composites. The combination of LZw and LiFSA represents an interesting matrix for electrochemical applications.

References

1. Electrochemical Aspects of Ionic Liquids; H. Ohno Ed., John-Wiley & Sons Inc., Hoboken, NJ, (2005).
2. P. Kubisa., *Prog. Polym. Sci.*, 29 (2004) 3.
3. H. Sakaebe, H. Matsumoto, K. Tatsumi, *J. Power Sources*, 146 (2005) 693.
4. A. I. Bhatt, A. S. Best, J. Huang, A. F. Hollenkamp, *J. Electrochem. Soc.*, 157 (2010) A66.
5. M. Yoshizawa-Fujita, D. R. MacFarlane, P. C. Howlett, M. Forsyth, *Electrochem. Commun.*, 8 (2006) 445.
6. (a) K. Hayamizu, Y. Aihara, H. Nakagawa, T. Nukuda, W. S. Price, *J. Phys. Chem. B*. 108 (2004) 19527, (b) T. Fromling, M. Kunze, M. Schonhoff, J. Sundermeyer, B. Roling, *J. Phys. Chem. B*, 112 (2008) 12985.
7. M. Yoshizawa-Fujita, N. Byrne, M. Forsyth, D. R. MacFarlane, H. Ohno, *J. Phys. Chem. B*, 49 (2010) 114.
8. (a) M. Yoshizawa, M. Hirao, K. Ito-Akita, H. Ohno, *J. Mater. Chem.*, 11 (2001) 1057; (b) M. Yoshizawa, A. Narita, H. Ohno, *Aust. J. Chem.*, 57 (2004) 139.
9. A. Narita, W. Shibayama, K. Sakamoto, T. Mizumo, N. Matsumi, H. Ohno, *Chem. Commun.*, (2006) 1926.
10. M. Yoshizawa-Fujita, T. Tamura, Y. Takeoka, M. Rikukawa, *Chem. Commun.*, 47 (2011) 2345.
11. P. Johansson, L. E. Fast, A. Matic, G. B. Appetecchi, S. Passerimi, *J. Power Sources*, 195 (2010) 2074.
12. H. Matsumoto, H. Sakaebe, K. Tatsumi, M. Kikuta, E. Ishiko, M. Kono, *J. Power Sources*, 160 (2006) 1308.
13. S. Seki, Y. Kobayashi, H. Miyashiro, Y. Ohno, Y. Mita, N. Terada, P. Charest, A. Guerfi, K. Zaghib, *J. Phys. Chem. C*, 112 (2008) 16708.
14. M. Biso, M. Mastragostino, M. Montanino, S. Passerini, F. Soavia, *Electrochim. Acta*, 53 (2008) 7967.
15. G. B. Appetecchi, M. Montanino, A. Balducci, S. F. Lux, M. Winter, S. Passerini, *J. Power Sources*, 192 (2009) 599.
16. M. Ishikawa, T. Sugimoto, M. Kikuta, E. Ishiko, M. Kono, *J. Power Sources*, 162 (2006) 658.
17. Y. Kato, M. Watanabe, K. Sanui, N. Ogata, *Solid State Ionics*, 40/41 (1990) 632.
18. J. Huang A. F. Hollenkamp, *J. Phys. Chem. C*, 114 (2010) 21840.
19. A. Narita, W. Shibayama, H. Ohno, *J. Mater. Chem.*, 16 (2006) 1475.
20. H. Lee, D. B. Kim, S.-H. Kim, H. S. Kim, S. J. Kim, D. K. Choi, Y. S. Kang J. Won, *Angew. Chem. Int. Ed.*, 43 (2004) 3053.
21. Y. Jin, S. Fang, L. Yang, S. Hirano, K. Tachibana, *J. Power Sources*, 196 (2011) 10658.

22. (a) H. Vogel, *Phys. Z.*, 22 (1921) 645, (b) G. S. Fulcher, *J. Am. Ceram. Soc.*, 8 (1925) 339, (c) G. Tamman, W. Hesse, *Z. Anorg. Allg. Chem.*, 156 (1926) 245.
23. (a) M. Hirao, H. Sugimoto, H. Ohno, *J Electrochem. Soc.*, 147 (2000) 4168; (b) H. Ohno M. Yoshizawa, *Solid State Ionics*, 154-155 (2002) 303.
24. B. Garcia, S. Lavallee, G. Perron, C. Michot, M. Armand, *Electrochim. Acta*, 49 (2004) 4583.
25. A. Hayashi, M. Yoshizawa, C. A. Angell, F. Mizuno, T. Minami, M. Tafsumisago, *Electrochem. Solid-State Lett.*, 6 (2003) E19.
26. F. M. Gray, Polymer Electrolytes, The Royal Society of Chemistry, London, (1997).
27. C. A. Angell, C. Lin, E. Sanchez, *Nature*, 362 (1993) 137.
28. H. Kim, D.Q. Ngyen, H.W. Bae, J.S. Lee, B.W Cho, H.S. Kim, M. Cheong, H. Lee, *Electrochem. Commun.*, 10 (2008) 1761.